

## CONCEPT OF SOIL TEMPERATURE COEFFICIENT FOR DETERMINING SPATIAL DISTRIBUTION OF SOIL TEMPERATURE, USING PHYSIOGRAPHIC PARAMETERS OF THE BASIN AND ARTIFICIAL NEURAL NETWORK (ANN)

Edyta Kruk<sup>1</sup>✉, Magdalena Malec<sup>1</sup>, Sławomir Klatka<sup>1</sup>, Andżelika Brodzińska-Cygan<sup>2</sup>

<sup>1</sup> Department of Land Reclamation and Environmental Development, Agriculture University of Krakow, al. Mickiewicza 24/28, 30-059 Kraków, Poland

<sup>2</sup> Philosophy Doctor Studies, Agriculture University of Krakow, al. Mickiewicza 24/28, 30-059 Krakow, Poland

### ABSTRACT

The paper presents the concept of soil temperature coefficient, as a ratio of soil temperature in the given point on the area of a basin and soil temperature in the basal point located within the watershed. For modelling the distribution of the soil temperature coefficient depending on selected soil and physiographic parameters, artificial neural networks (ANN) were used. ANN were taught based on empirical data, which covered measurements of soil temperature in 126 points, in the layer of soil at the depth of 0–10 cm, within the area of the Małny stream basin located in the Gorce mountain range of West Carpathians. The area size of the basin amounts to 1.47 km<sup>2</sup>. Temperature was measured by means of a TDR device. The soil and physiographic parameters included: slopes, flow direction, clay content, height above sea level, exposition, slope shape, placement on the slope, land-use, and hydrologic group. Parameters were generated using DEM of 5m spatial resolution and soil maps, using the ArcGIS program. The MLP 10-8-1 model proved to be the best fitted neural network, with 8 neurons in the hidden layer. The quality parameters were satisfactory. For the learning set, the quality parameter amounted to 0.805; for the testing set, 0.894; and for the validating set, 0.820. Global sensitivity analysis facilitated the assessment of percentage shares, contributing to the soil temperature ratio. Land use (25.0%) and exposition (20.5%) had the highest impact on of the aforementioned ratio, while the placement on the slope and flow direction had the lowest impact.

**Key words:** soil temperature, basin physiographic parameters, artificial neural networks (AAN)

### INTRODUCTION

Heat is one of the essential soil factors, which impact plant life, apart from water conditions, nutrients, and air. The main source of soil heat is solar energy. Its amount entering the Earth's surface depends on many factors, including geographical position, climate, time of day, and season of the year. Topographic features, especially exposition, slopes, plant cover, texture, and wetness are significant as well [Scriboon 2017, Dutta

et al. 2018]. Secondary sources of soil heat include: warm winds, heat from precipitation, heat inside the Earth, heat from soil processes, heat released at wetting dry soil, and radioactivity. The most essential parameters characterizing soil heat properties are: thermal capacity (specific heat), thermal conductivity, and ability of soil to heat. The basic indicator of heat relations, as well as resultant of many of its properties, is temperature. Soil temperature is characterized by natural repeatability in daily [Scriboon et al. 2017]

✉ e-mail: e.kruk@ur.krakow.pl

and yearly cycles [Bryś 2004, Bryś 2008]. The highest values and amplitude during the day is registered near soil surface. With the depth increase, the amplitude decreases, and finally it disappears [Scriboon et al. 2017]. The depth of disappearance depends in particular on soil thermal conductivity. Multiyear observations show that the depth of daily temperature fluctuations disappearance amounts to dozens of centimetres, while in the case of yearly fluctuations, this depth reaches between several and over a dozen centimetres. Daily course of temperature oscillation depends on the weather on a given day and season of the year, while the annual temperature oscillation is shaped by the climate of the given area [Kunkel 2016]. Distribution of soil temperature depends on physiographic conditions, water content, plant cover, and human activity [Turski et al. 1984, Zawadzki 1999, Klatka et al. 2015, Malec et al. 2015, Boroń et al. 2016]. In this work, we have analysed the concept of soil temperature ratio, as a value for a particular point within the basin area, depending upon chosen physiographic parameters, using artificial neural network (ANN), applied, inter alia, in the modelling of various soil properties and their spatial distribution [Minasny et al. 1999, Merdun et al. 2006, Wang et al. 2012, Patil and Singh 2016, Halecki et al. 2017].

## STUDY AREA

The investigated area covers the Małny stream basin, of 1.47 km<sup>2</sup> area in the southern part of the Małopolska region. The basin is situated in Southern Poland, in the administrative district Limanowa, within Mszana Dolna and Niedźwiedź municipalities (see: Figure 1). According to Kondracki's *Geografia regionalna Polski (Regional geography of Poland)* [Kondracki 2009], taking into account physico-geographical regionalization of Europe, the area of the basin belongs to Western Europe. Regarding location against the background of configuration and geological structure of Europe, the area of the basin should be classified as physico-geographical province of Western Carpathians. The external part of Western Carpathians, the Magurka, built of several overlapping structures from the South, consisted of alternately located sandstones, conglomerates and Paleogene and Cretaceous slates (flysch), subjected to decay by erosion and denudation. Mean elevation of the catchment above sea level was 582.66 m. The montane and sub-montane climate is characterized by large contrasts within the local climate, which is rather cold, with a considerable amount of rainfall. Floods, occasionally disastrous, occur twice a year (in

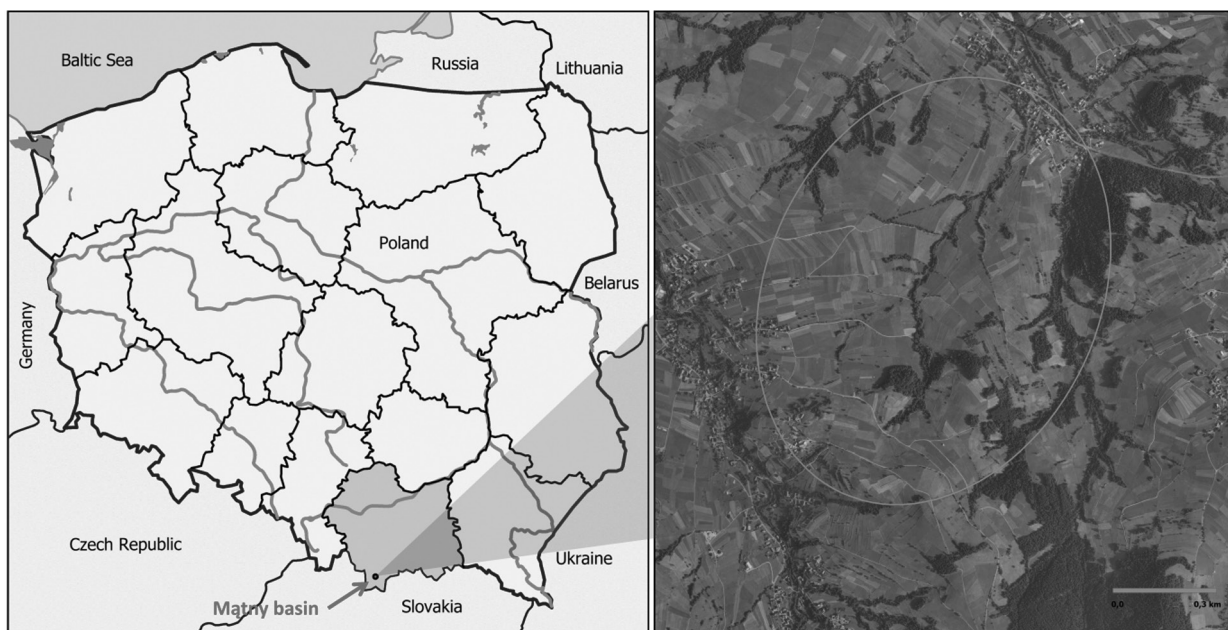


**Fig. 1.** Location of the research area within the territory of Poland

spring and in summer). In the year 2014, mean annual air temperature was 7.4°C, and the annual average total precipitation was 948.1 mm. The highest daily precipitation was 100.7 mm on 15 May 2014.

Soils within the basin area were created as a result of weathering of sandstones, conglomerates and slates. In Table 1 we have presented soil granular groups [Kruk 2016]. The soil cover in the Małny stream catchment is dominated by loamy soils, including sandy clay loam (36.1%), loam (36.1%), silt loam (23.1%), clay loam (4.1%), and sandy loam (0.6%). Pedological conditions were identified by the analysis of a 1:25000 agricultural soil map, and qualified in the respective groups according to USDA standards (Soil Survey Staff, 1975) [Halecki et. al. 2018a, b].

## MATERIAL AND METHODS

Relative soil temperature coefficient  $K_t$  was determined based on the concept of wetness coefficient [Svetlitchnyi et al. 2003]:

$$K_w = \frac{\Theta_v}{\Theta_{v,b}}$$

where:

- $\Theta_v$  – soil volumetric water content in the given point within the basin area,  $m^3 \cdot m^{-3}$ ,
- $\Theta_{v,b}$  – soil volumetric water content in the basal point,  $m^3 \cdot m^{-3}$ .

Similarly, in the present work we propose soil temperature coefficient  $K_t$  calculated as:

$$K_t = \frac{t_i}{t_{i,b}}$$

where:

- $t_i$  – soil temperature in the given point within the basin area, °C,
- $t_{i,b}$  – soil temperature in the basal point, °C.

The purpose of the  $K_t$  is to assess distribution of soil temperature in the catchment area, based on the measurement in the basal point, located on a hilltop.

Soil temperature and moisture was measured using the TDR device, as a mean value in 0–0.10 m layer in 126 measuring points (see: Figure 2) on 29 September 2014 (between 11 pm and 14 am), during the day without any rainfall. Distribution of points was random,

taking into account the specific character of the mountain catchment.

Topographic parameters were determined based on a 1 : 5000 topographic map and a Digital Elevation Model with spatial resolution of 5 m. Data was generated using the MapInfo Professional and ArcGIS. The following parameters were determined: altitude, slope, water flow direction, exposition, shape of the slope, and situation on the slope.

**Altitude** [m a.s.l.] – was determined using DEM.

**Slope** – as local value, was determined as:

$$S = \frac{\Delta h}{l} \cdot 100\%$$

where:

- $l$  – length of projection of direction between the points, m,
- $\Delta h$  – differences of heights between the points, m.

In the present study, the slopes were determined using the Surfer in six intervals: 0–5%, 5–10%, 10–18%, 18–27% and >27%.

**Flow direction** – was determined based on height difference between the given cell determined using DEM, and each of the 8 adjacent cells, based on one-direction point model D8. Calculations were carried out according to Wilson and Gallant [2000]:

$$S_{D8} = \max_{i=1,8} \frac{Z_9 - Z_i}{h\varnothing(i)}$$

where:

- $Z$  – number of adjacent cell,
- $h$  – resolution of the GRID model,
- $h\varnothing(i)$  – distance between the middle points of cells,
- $1$  – for the ones situated in basic directions (N, E, S, W), root square for the two remaining ones.

**Exposition** – location on the slope with respect to the direction of sunlight rays, determined in 4-grade scale, as one of the geographical directions (E – east, W – west, N – north and S – south).

**Shape of the slope** – was determined as: concave, flat, or convex.

**Situation on a slope** – was determined in 5-grade scale, based on DEM, according to scheme presented on Figure 3.

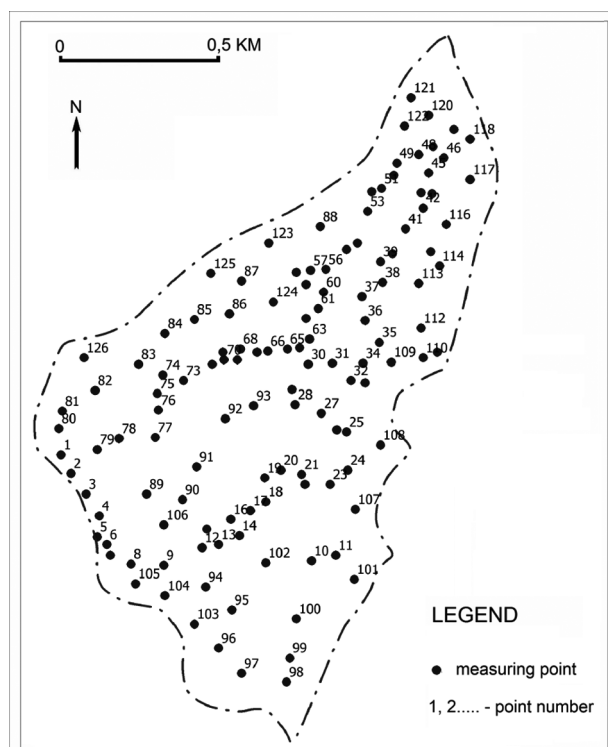


**Fig. 2.** Situation of measuring points within the area of the basin

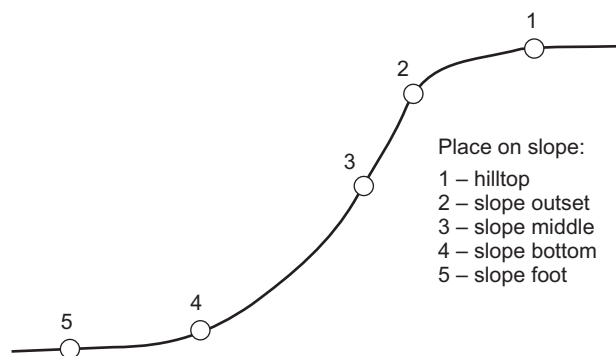


**Fig. 3.** Diagram for determining the situation of measuring points on a slope

**Clay fraction** was determined by means of the Cassagrande method [Oleksynowa et al. 1993].

**Use** – was determined based on the 1:1000 orthophotomap and verified based on field observation.

**Hydrological group** – was determined based on the method proposed by U.S. Department of Agriculture – Natural Resources Conservation Service. In this

method, soils are classified to one of the four groups A, B, C, and D regarding water permeability. Characterization of hydrological group was presented in [USDA... 2002, Kruk 2016, Ryczek 2011].

For soil temperature coefficient, the ANN (Artificial Neural Network) approach was used, with a hyperbolic tangent (tanh) function applied to activate the hidden and the output layers. A multilayer perceptron was used to analyse the variables. A total of 70% of all variables were applied for the learning process; 15% were used for the validation, and further 15%, to test the model. A quasi-Newton algorithm with a BFGS (Broyden-Fletcher-Goldfarb-Shanno) modification was selected for the learning neural network. Sum of squares (SOS) was treated as the error function. The ANN model was used with the objective of establishing the association between the soil temperature coefficient, whereas physiographic parameter, indicative of the soil and its use, was applied in all data sets as independent variable. Statistical software ver. 12.5 was used to build the ANN architecture. The multi-layer perceptron consisted of three layers of neurons: the input layer, the output layer, and the hidden layer (Dawson et. al., 2006, Halecki et al. 2018c).

The analysis of the empirical model's adjustment to experimental data was carried out by means of the following measures [Rahnama i Barani 2005]:

- mean error of prognosis (*MEP*)

$$MEP = \frac{1}{n} \cdot \sum_{i=1}^n (C_i^m - C_i^p)$$

- root of mean square error (*RMSE*)

$$RMSE = \sqrt{\frac{1}{n} \cdot \sum_{i=1}^n (C_i^m - C_i^p)^2}$$

- mean percentage error (*MPE*)

$$MPE = \frac{1}{n} \cdot \sum_{i=1}^n \frac{C_i^m - C_i^p}{C_i^m} \cdot 100\%$$

- model efficiency (*ME*) [Nash and Sutcliffe 1970]

$$ME = 1 - \frac{\sum_{i=1}^n (C_i^m - C_i^p)^2}{\sum_{i=1}^n (C_i^m - C)^2}$$

where:

- $C_i^m$  – measured values
- $C_i^p$  – simulated values
- $n$  – number of data

## RESULTS AND DISCUSSION

Temperature in the base point amounted to 13.2°C. The measured temperatures fluctuated between 12.0°C and 15.2°C. Based on the results of the investigation of physiographic parameters, the ANN model was generated. The best fitted model turned out to be the MLP 10-8-1, with 8 perceptrons in the hidden layer (see: Figure 4). The MLP 10-8-1 model is characterized by high values of fitting quality and low error, and therefore it presents good adjustment (see: Table 1). Thanks to global sensitivity analysis (see: Table 2), the relative and absolute influence of a number of parameters on the soil temperature coefficient  $K_t$  were determined. In the Małny stream basin, the following parameters had the highest impact: land use (25.0%) and exposition (20.5%) (see: Table 2). Based on the simulated values of the soil temperature coefficient for every of the measured points, the map of spatial distribution of this parameter was generated using the Surfer 10 and Arc-

GIS (see: Figure 5). Values of the soil temperature coefficient fluctuated between 0.91 and 1.13. The highest values of the soil temperature coefficient occurred in north-west part of the basin. Figure 6 presents comparison between the simulated and the measured values of soil temperature coefficient. Figure 7 presents spatial distribution of simulated temperature coefficient generated by ANN 10-8-1. Values of the simulated temperature coefficient remained in the range between 0.89 and 1.13.

**Table 1.** Analysis of quality and errors of the MLP 10-8-1 model

Quality	learning	0.805
	testing	0.894
	validation	0.820
Error	learning	0.001
	testing	0.001
	validation	0.001
Perceptron activation functions	hidden	tanh
	output	tanh

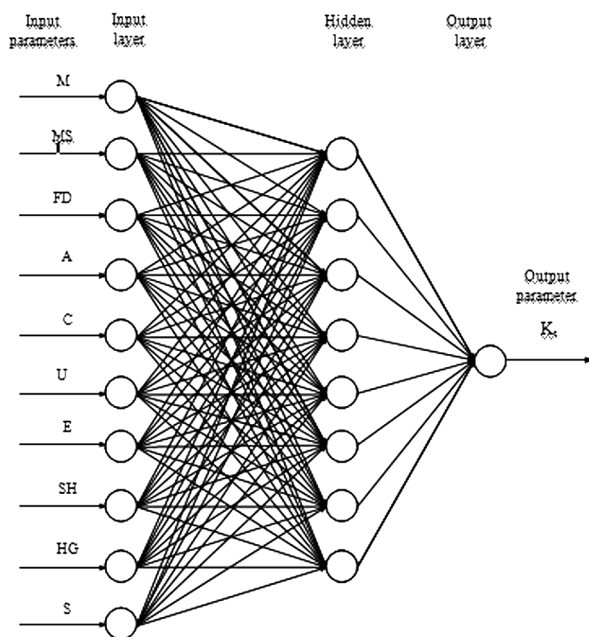


**Fig. 4.** Diagram of the MLP 10-8-1 model

**Table 2.** Global sensitivity analysis of the MLP 10-8-1 model

Nb	Parameter	Relative sensitivity, –	Absolute influence, %
1	Use (U)	3.745504	25.0
2	Exposition (E)	3.072321	20.5
3	Altitude (A)	1.080924	7.2
4	Shape of the slope (SH)	1.038404	6.9
5	Clay content (C)	1.023403	6.8
6	Moisture (M)	1.021369	6.8
7	Slope (S)	1.004643	6.7
8	Hydrological group (HG)	1.000000	6.7
9	Flow direction (FD)	0.997832	6.7
10	Situation on a slope (MS)	0.996385	6.7

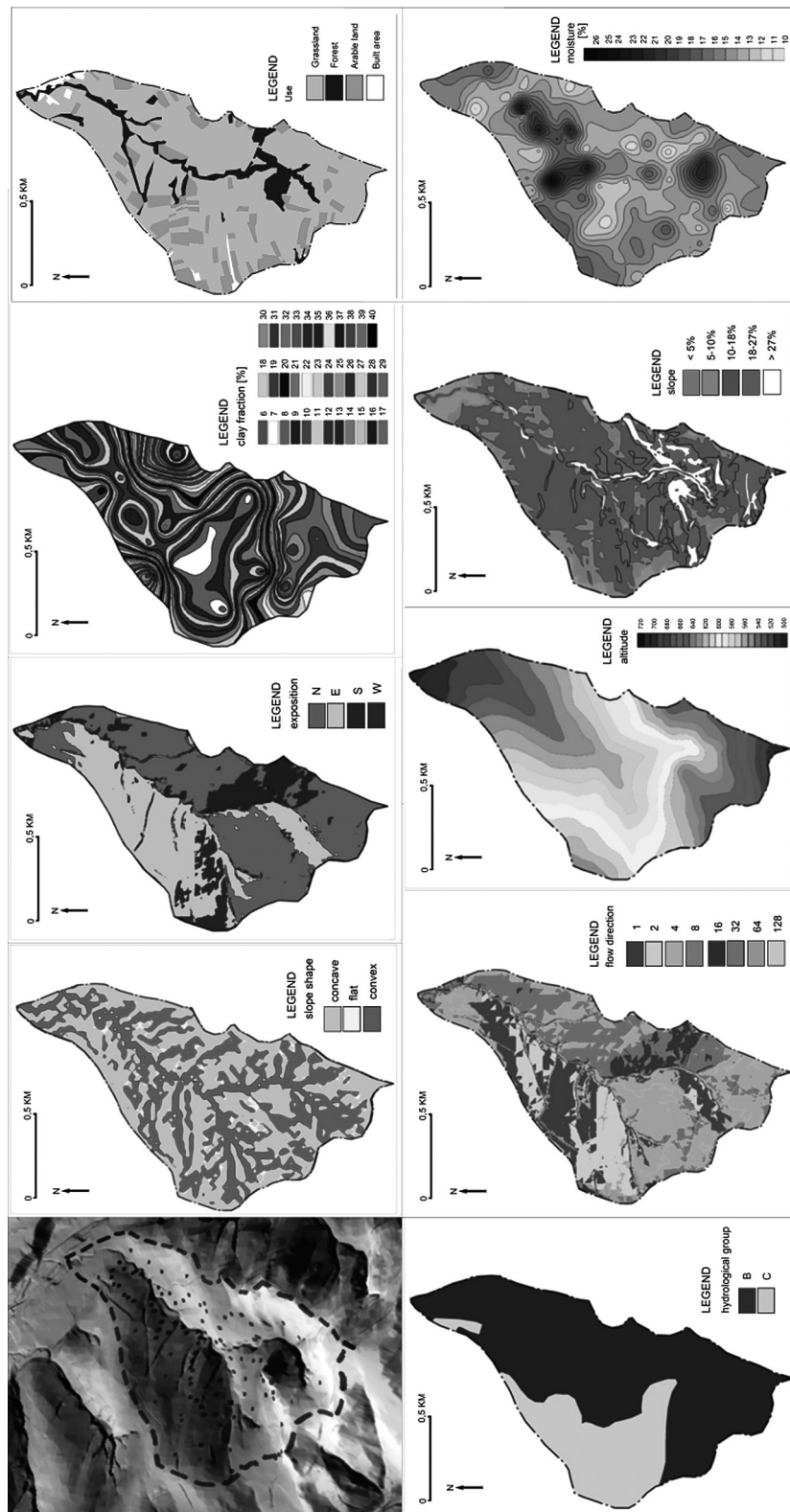


**Fig. 5.** Maps of physiographic parameters within the Małny stream basin.

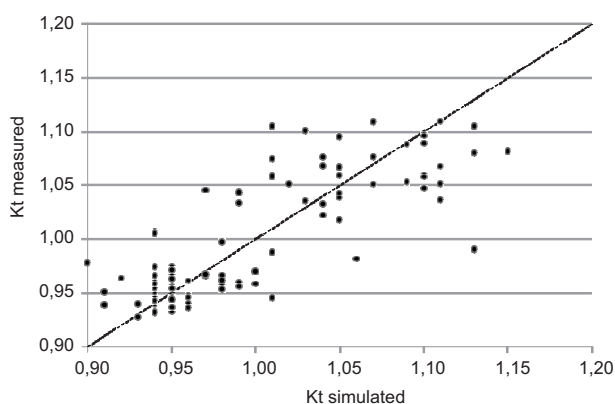


**Fig. 6.** Measured versus simulated soil temperature coefficient

**Table 3.** Model efficiency measures for the MLP 10-8-1

Model efficiency measures				
MEP, –	RMSE, –	MPE, %	ME, –	r, –
–0.001	0.039	–0.256	0.65	0.820

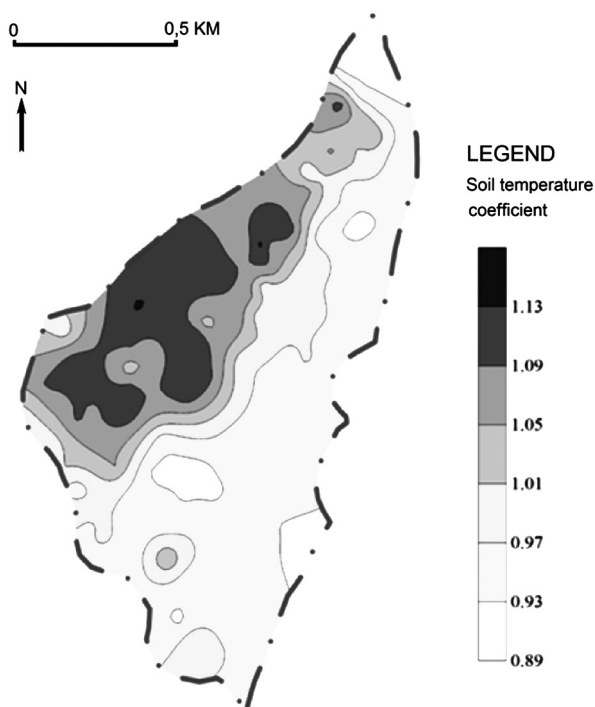


**Fig. 7.** Spatial distribution of the soil temperature coefficient in the Małny stream basin generated using the MLP 10-8-1 model

## CONCLUSIONS

1. Global sensitivity analysis of the MLP 10-8-1 model has demonstrated that the highest influence on soil temperature coefficient comes from exposition and land use, whereas the hydrological group had the lowest impact.
2. Model efficiency measures show good adjustment between the values of soil temperature coefficient simulated using the MLP 10-8-1 model and the experimental data. Low overestimation of data was noticed.
3. The proposed concept of soil temperature coefficient facilitates the modelling of soil temperature distribution, using measurement in one point and physiographic parameters.

## REFERENCES

- Boroń, K., Klatka, S., Ryczek, M., Liszka, P. (2016). Kształtowanie się właściwości fizycznych, fizykochemicznych i wodnych rekultywowanego i niezrekultywowanego osadnika byłych Krakowskich Zakładów Sodowych „Solvay”. *Acta Sci. Pol., Formatio Circumiectus*, 15(3), 35–43.
- Bryś, K. (2004). Wieloletnia zmienność termiki gleby we Wrocławiu-Swojcu i jej radiacyjne i cyrkulacyjne uwarunkowania. *Acta Agrophysica*, 3(2), 209–219.
- Bryś, K. (2008). Wieloletni wpływ pokrywy roślinnej na termikę gleby. *Acta Agrophysica*, 12(1), 39–53.
- Dawson, C.W., Abraham, R.J., Shamseldin, A.Y., Wilby, R.L. (2006). Flood estimation at ungauged sites using artificial neural networks. *J. Hydrol.*, 319, 391–409
- Dutta, B., Grant, B.B., Congreves, A., Smith, W.N., Wagner-Riddle, C., VanderZaag, A.C., Tenuta, M., Desjardins, R.L. (2018). Characterising effects of management practises, snow cover, and soil texture on soil temperature: Model development in DNDC. *Science Direct*, 168, 54–72.
- Halecki, W., Młyński, D., Ryczek, M., Radecki-Pawlik, A. (2017). The Application of Artificial Neural Network (ANN) to Assessment of Soil Salinity and Temperature Variability in Agricultural Areas of a Mountain Catchment. *Polish J. Environ. Stud.*, 26(6), 1–10.
- Halecki, W., Kruk, E., Ryczek, M. (2018a). Evaluation of soil erosion in the Małny stream catchment in the West Carpathians using the G2 model. *Catena*, 16, 116–124.
- Halecki, W., Kruk, E., Ryczek, M. (2018b). Influence of various use scenarios on soil loss in the Małny stream

- catchment in the Gorce, West Carpathians region. *Land Use Policy*, 73, 363–372.
- Halecki, W., Kruk, E., Ryczek, M. (2018c). Estimations of nitrate nitrogen, total phosphorus flux and suspended sediment concentration (SSC) as indicators of surface erosion processes using an ANN (Artificial Neural Network) based on geomorphological parameters in mountainous catchments. *Ecological Indicators*, 91, 461–469.
- Klatka, S., Malec, M., Ryczek M., Boroń K. (2015). Wpływ działalności eksploatacyjnej Kopalni Węgla Kamiennego „Ruch Borynia” na gospodarkę wodną wybranych gleb obszaru górniczego. *Acta Sci. Pol., Formatio Circumiectus*, 14(1), 115–125.
- Kondracki, J. (2009). *Geografia regionalna Polski*. Wydawnictwo Naukowe PWN, Warszawa.
- Kruk, E. (2016). Zastosowanie technik GIS w ocenie zagrożenia erozją wodną na przykładzie zlewni potoku Mątny w Beskidzie Wyspowym. Praca doktorska. Uniwersytet Rolniczy w Krakowie (unpublished).
- Kunkel, V., Wells, T., Hanckooock, G.R. (2016). Soil temperature dynamics at the catchment scale. *Geoderma*, 273, 32–44.
- Malec, M., Klatka, S., Ryczek, M. (2015). Wpływ antropopresji na dynamikę wzrostu warstwy akrotelmowej na torfowisku wysokim Baligłówka w Kotlinie Orawsko-Nowotarskiej. *Acta Sci. Pol., Formatio Circumiectus*, 14(1), 149–161.
- Merdun, H., □mar, □, Meral, R., Apan, M. (2006). Comparison of artificial neural networks and regression pedotransfer functions for predictions of soil water retention and saturated hydraulic conductivity. *Soil & Tillage Research*, 90, 108–116.
- Minasny, B., McBratney, A.B., Bristow, K. (1999). Comparison of different approaches to the development of pedotransfer functions for water-retention curves. *Geoderma*, 93, 225–253.
- Nash, J.E., Sutcliffe, J.V. (1970). River flow forecasting through conceptual models. Part I. A discussion of principles. *J. Hydrol.*, 10, 282–290.
- Oleksynowa, K., Tokaj, J., Jakubiec, J. (1993). *Przewodnik do ćwiczeń z Gleboznawstwa i Geologii. Część II: Metody laboratoryjne analizy gleby*. Akademia Rolnicza, Kraków.
- Patil, N., Singh, S.K. (2016). Pedotransfer functions for estimating soil hydraulic properties. A review. *Pedosphere*, 26(4), 417–430.
- Rahnana, M.B., Barani, G.A. (2005). Application of rainfall-runoff models to Zard river catchment. *American J. Environm. Sci.*, 1(1), 86–89.
- Ryczek, M. (2011). Prognozowanie natężenia transportu rumowiska unoszonego w małych ciekach górskich Karpat Zachodnich z wykorzystaniem parametrów fizjograficznych zlewni. *Zesz. Nauk. UR Kraków*, 477, Rozprawy, 354.
- Scriboon, W., Tuntiwaranuruk, U., Sanoamuang, N. (2017). Hourly soil temperature and moisture content variations within a concrete pipe container for planting lime trees in Eastern Thailand. *Case Studies in Thermal Engineering*, 10, 192–198.
- Svetlitchnyi, A.A., Plotnitskiy, S.V., Stepovaya, O.Y. (2003). Spatial distribution of soil moisture content within catchments and its modeling on the basis of topographic data. *J. Hydrol.*, 277, 50–60.
- Turski, R., Słowińska-Jurkiewicz, A., Hetman, J. (1984). *Zarys gleboznawstwa*. PWN, Warszawa.
- USDA (2002). *National Soil Survey Hand-book*, title 430-VI, US Department of Agriculture, Natural Resources Conservation Service.
- Wang, G., Zhang, Y., Yu, N. (2012). Prediction of soil water retention and available water of sandy soils using pedotransfer functions. *Procedia Engineering*, 37, 40–53.
- Wilson, D.J., Gallant, J.C. (2000). *Digital terrain analysis*. [In:] D.J. Wilson, J.C. Gallant (eds.). *Terrain Analysis: Principles and Applications*. John Willey & Sons, INC, New York, 1–27.
- Zawadzki S. 1999. *Gleboznawstwo*. PWRiL, Warszawa.

## KONCEPCJA WSPÓŁCZYNNIKA TEMPERATURY GLEBY DO WYZNACZANIA ROZKŁADU PRZESTRZENNEGO TEMPERATURY GLEBY Z WYKORZYSTANIEM PARAMETRÓW FIZJOGRAFICZNYCH ZLEWNI I SZTUCZNYCH SIECI NEURONOWYCH (SSN)

### ABSTRAKT

W pracy zaprezentowano koncepcję współczynnika temperatury gleby, jako ilorazu temperatury gleby w danym punkcie w zlewni i temperatury w punkcie bazowym zlokalizowanym na wododziale. Do modelowania rozkładu współczynnika temperatury gleby w zależności od wybranych parametrów fizjograficznych

i glebowych wykorzystano sztuczne sieci neuronowe (SSN). SSN została nauczona w oparciu o dane empiryczne, obejmujące pomiary temperatury gleby, w warstwie 0–10 cm w 126 punktach, na terenie zlewni potoku Małny zlokalizowanej w Gorcach, w Karpatach Zachodnich. Powierzchnia zlewni wynosi 1,47 km<sup>2</sup>. Temperatura była mierzona za pomocą urządzenia typu TDR. Parametry glebowe i fizjograficzne objęły: kierunek spływu, zawartość ilu, wysokość n.p.m., ekspozycję, kształt stoku, położenie na stoku, użytkowanie terenu i grupę hydrologiczną gleby. Parametry zostały wygenerowane przy użyciu NMT o rozdzielczości 5 m i mapy glebowo-rolnicze, przy użyciu programu ArcGIS. Najlepiej dopasowanym modelem sztucznych sieci neuronowych okazał się model MLP 10-8-1, z 8 neuronami w warstwie ukrytej. Parametry jakości dopasowania sieci były satysfakcjonujące. Parametr jakości dla zbioru uczącego wyniósł 0,805, dla testowego 0,894 i dla walidacyjnego 0,820. Globalna analiza wrażliwości sieci pozwoliła na ocenę procentowego udziału poszczególnych parametrów wyjaśnianiu kształtowania się wartości współczynnika temperatury gleby. Największy wpływ miały: użytkowanie terenu (25,0%) i ekspozycja (20,5%), a najmniejszy położenie na stoku oraz kierunek spływu wody.

**Słowa kluczowe:** temperatura gleby, parametry fizjograficzne zlewni, sztuczne sieci neuronowe (SSN)